Supporting Information

Structural Design Considerations of Solution-Processible Graphenes as Interfacial Materials via Controllable Synthesis to Achieve Highly Efficient, Stable, and Printable Planar Perovskite Solar Cells

Jun-Seok Yeo,[a] You-Hyun Seo,[b] Chan-Hee Jung,[c] and Seok-In Na*[b]

[a]Carbon Convergence Materials Research Center, Institute of Advanced Composite Materials, Korea Institute of Science and Technology, 92 Chudong-Ro, Bongdong-eup, Wanju-gun, Jeonbuk 55324, Republic of Korea

[b]Professional Graduate School of Flexible and Printable Electronics, Polymer Materials Fusion Research Center, Chonbuk National University, 664-14, Deokjin-dong, Deokjin-gu, Jeonju-si, Jeollabuk-do, 54896, Republic of Korea
E-mail: nsi12@jbnu.ac.kr

[c]Research Division for Industry and Environment, Korea Atomic Energy Research Institute, 29 Geumgu-gil, Jeongeup-si, Jeollabuk-do 580-185, Republic of Korea

Experimental Section

Functionalization of graphene oxides (FGOs): GOs were prepared by the previously reported route.[27] To fuctionalize styryl groups on GOs (FGOs), a *N*,*N*'-diisopropylcarbodiimide (DIC, Sigma Aldrich)-mediated coupling reaction between -COOH moieties on as-prepared GOs and -NH_2 moieties on 4-aminostyrene was used. First, 1.0 g of GO was dispersed in 200 ml of *N*,*N*-dimethylformamide (DMF, Sigma Aldrich) for 0.5 h under ultrasonication, followed by addition of 15 g of DIC. Then, 4 g of 4-aminostyrene (Tokyo Chemical) was dissolved in 10 ml of DMF and stirred for 4 h. The two prepared solutions were mixed and stirred for 24 h at room temperature. Finally, resultant products were collected through filtration, and repeatedly washed by DMF and ethanol (EtOH, Sigma Aldrich), and dried in a vacuum oven for 24 h.

Preparation of polyacrylonitrile-grafted reduced GO (PRGO): The prepared FGO (1.0 g) was dispersed in DMF (800 ml), and then, acrylonitrile (AN, Showa Company) as a precursor for grafting was added at various concentrations (1, 2, 4, and 6 wt%) into the FGO solution. The mixed solution in a glass bottle was sealed with a rubber cap and purged with nitrogen gas to remove oxygen. For in-situ graft polymerization and reduction of FGO, the prepared solution in a glass bottle was irradiated by gamma rays from a ^{60}Co source at room temperature in the Advanced Radiation Technology Laboratory (ARTI) of the Korea Atomic Energy Research Institute (KAERI). The total absorbed dose was modulated from 200 to 600 kGy with a constant dose rate (10 kGy/h). Next, the reactant in the solution was precipitated with methanol (MeOH, Showa Company). The precipitated reactant (PRGO) was collected by filtration, and repeatedly washed with DMF and EtOH, and dried at vacuum oven for 24 h. In

addition, for reference experiments, radiation-reduced styryl-functionalized GO (RFGO) was also prepared by the same reduction procedure as PRGO except for AN addition, where in the case of RFGO, the AN was not added.

Characterization of materials: Ultraviolet-visible (UV–vis) spectra (absorbance and transmittance modes) were recorded by a Scinco S-3100 spectrophotometer. Dispersibilities of various graphene derivatives in DMF solvents were evaluated by plotting the UV-Vis absorbance at 269 nm as a function of their concentrations (1, 2, 5, and 10 mg L^{-1}). Fourier-transform infrared (FTIR) spectra were obtained by a Varian 640 spectrometer equipped with an attenuated total reflectance (ATR) unit with a ZnSe crystal. X-ray photoemission spectroscopy (XPS) and ultraviolet photoemission spectroscopy (UPS) (AXIS NOVA, Kratos) measurements were carried out using a monochromatized Al Kα for XPS, and a He I (hv = 21.2 eV) excitation for UPS at a pressure of 5×10^{-8} torr. Reference gold was used for the accurate detection of Fermi energy for the UPS analysis. X-ray diffraction (XRD) patterns were collected by a Rigaku Micromax-002 diffractometer with a Cu Kα (λ = 0.1542 nm) source. A scanning electron microscope (NOVA NanoSEM 450, FEI) and an atomic force microscope (Dimension 3100, Veeco) with a tapping mode were used for characterization of the film morphologies. Raman spectra were obtained from an AM-HR 800 spectrometer with an excitation laser source (514 nm). Electrical conductivities of samples on glass substrates were measured using a 4-point probe conductivity meter (Advanced Instrument Technology). Contact angles of samples on glass/ITO substrates were collected by using a Phoenix 300. Measurements of time-resolved photoluminescence (TRPL) were performed by the second harmonic generation (at 400 nm) of a mode-locked Ti:Sapphire laser

(Chameleon Ultra II, Coherent) with a pulse duration of 150 fs equipped with an external pulse-selector (9200 series, Coherent Inc.). To reduce the repetition rate at 3.6 MHz, fluorescence radiation was spectrally filtered with a narrow bandwidth and focused on the entrance slit of a 300 mm spectrometer (Acton Spectra Pro 2300i, Princeton Instruments) at a spectral resolution of about 1 nm. PL lifetime was collected using a picosecond streak camera (C11200, Hamamatsu Photonics). 2D grazing incident wide-angle X-ray scattering (GIWAXS) measurement was carried out with a synchrotron source at 5A beamline at the Pohang Accelerator Laboratory in Korea. The wavelength of the incident X-ray was 1.0716 Å with a fixed incident angle of 0.13°.

Fabrication of perovskite solar cells (PeSCs): For device-fabrication, all garphene derivatives used in this study (except for RFGO due to its low dispersibility) were dispersed in DMF at a concetration of 10 mg ml^{-1}. First, patterned glass/ITO (140 nm, 15 Ω $□^{-1}$) were UV/O_3-treated for 30 min. Various HTLs including PEDOT:PSS (Clevios™ P VP AI 4083, Heraeus), GO, FGO, RFGO, and PRGO were spin-coated onto the prepared substrates at 5000 rpm for 40 s, and then, the films were annealed at 150 °C for 10 min. For one-step deposition of perovskite film, a perovskite precursor solution (35 wt%) was prepared by dissolving CH_3NH_3I (MAI, Dyesol) and PbI_2 (Alfa Aesar) in a 1:1 molar ratio in a DMF solvent. After stirring for 12 h at 60 °C in a N_2-filled glovebox, 7 vol% of N-cyclohexyl-2-pyrrolidone (CHP, Sigma Aldrich) was added to the resulting precursor solution. The premixed perovskite precursor solution was spin-coated onto the respective HTLs at 6000 rpm for 90 s without any quenching processes, followed by annealing at 100 □C for 2 min. Next, $PC_{61}BM$ (Nano-C) dissolved in chlorobenzene (CB, Sigma Aldrich) with a concentration of 20 mg ml^{-1} was spin-

coated onto the perovskite film at 1000 rpm for 60 s without additional heat treatments. Finally, top electrodes of bathocuproine (BCP, Alfa Aesar) (3 nm)/Ag (80 nm) were thermally deposited onto the $PC_{61}BM$ layer through a shadow mask (active area: 4.64 mm^2) at a pressure of 1×10^{-6} torr. For fully printed PeSCs, HTLs were deposited on glass/ITO substrates via slot-die system at a coating speed of 4 mm s^{-1} and a solution feed of 35 µL min^{-1} at 50 °C, and then, the films were annealed at 150 °C for 10 min. Next, the perovskite precursor solution was coated by slot-die with the optimized condition. The $PC_{61}BM$ solution was slot-die coated at a coating speed of 7 mm s^{-1} and a solution feed of 35 µL min^{-1} at 40 °C. Finally, BCP (3 nm)/Ag (80 nm) cathodes were deposited under a vacuum of 1×10^{-6} torr.

Characterization of PeSCs: Photocurrent density-voltage (J-V) characteristics of the PeSCs were obtained with a Keithley 2400 source unit and Oriel Class AAA solar simulator under 100 mA cm^{-2} illumination from AM 1.5 G sunlight. A calibrated silicon cell (SRC-1000-TC-KG5-N, VLSI Standards. Inc) was used as a reference cell for accurate measurement. EQE and IQE of the PeSCs were simultaneously collected via an Oriel® IQE-200 QE Measurement System. For device-stability estimation, photovoltaic performances of the PeSCs were recorded as a function of storage time (according to the ISOS-D-1 protocol [44]) at ambient conditions (humidity of ~50%, temperature of ~25 °C) without encapsulation.

Capacitance-voltage (C-V) data were obtained by using Agilent 4284A precision LCR meter with Keithley 4200-SCS setup at a fixed frequency of 10 kHz under a dark condition. AC oscillating voltage was maintained at 20 mV to obtain a linear response.

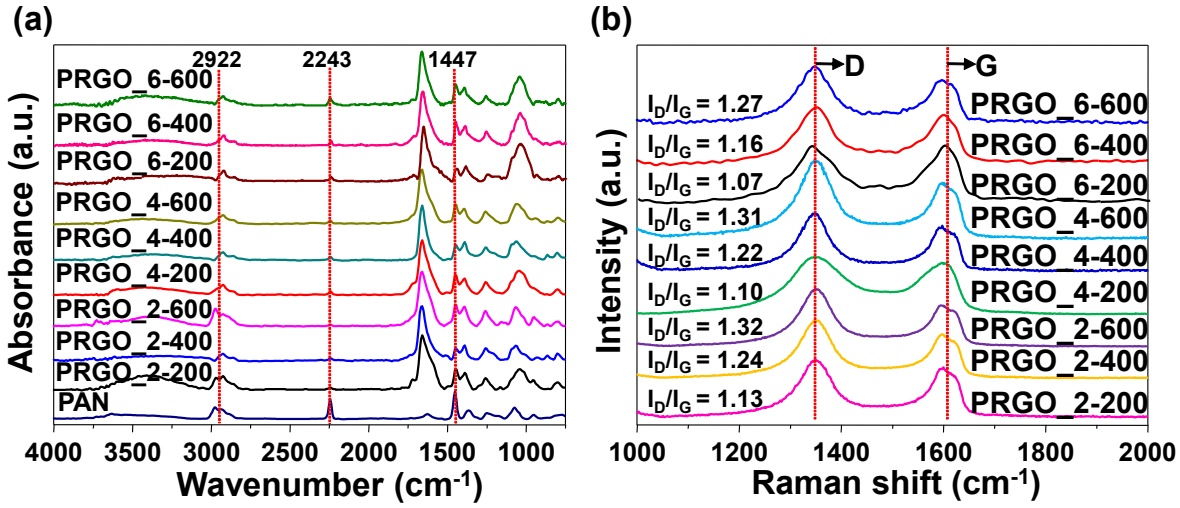

Fig. S1. (a) FTIR spectra and (b) Raman G-band spectra of various PRGOs.

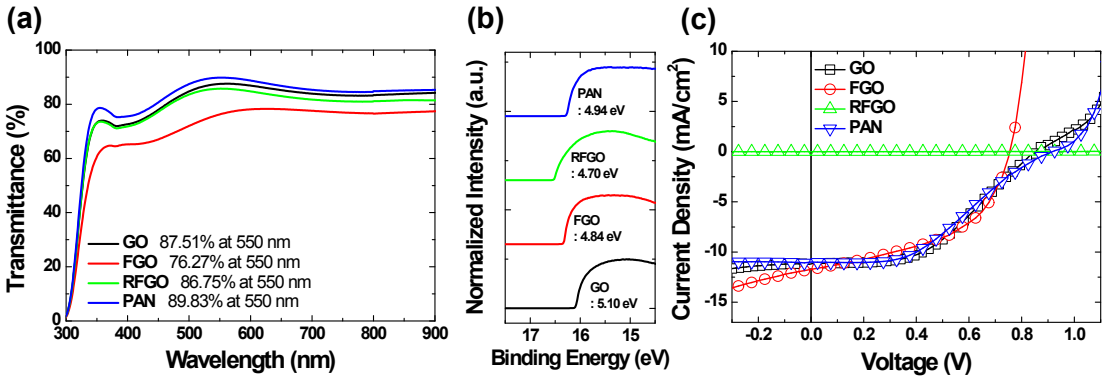

Fig. S2. (a) Transmittance and (b) UPS spectra in secondary electron cutoff region of ITO/GO, ITO/FGO, ITO/RFGO, and ITO/PAN. (c) Corresponding J-V curves of PeSCs.

Fig. S2 shows that both the grafted PAN and the template of the reduced graphene oxide are required for the PRGO HTL to be effectively used in PeSCs. All the devices with HTLs including GO, FGO, RFGO, and PAN exhibited significantly poor photovoltaic characteristics. The devices based on the GO and FGO showed poor PCEs in the range of 3~4%, probably due to the highly oxygenated surfaces of the GO and FGO. These oxygen moieties on the graphene sheets are essential to disperse graphene derivatives in solvents for solution-process, but these oxygen moieties could activate the recombination between photo-generated charge carriers, thereby leading to the performance degradation observed in the PeSCs. In addition, it is surprising that the RFGO device failed to show the photovoltaic characteristics despite the favorable conductivity and WF of the RFGO. As observed in Fig. 2b, the RFGO without the grafted PAN had very poor dispersibility, which resulted in quietly irregular surface of the resultant rGO film. In the case of the pristine PAN, the device was also inefficient mostly due to the insulating property of the PAN.

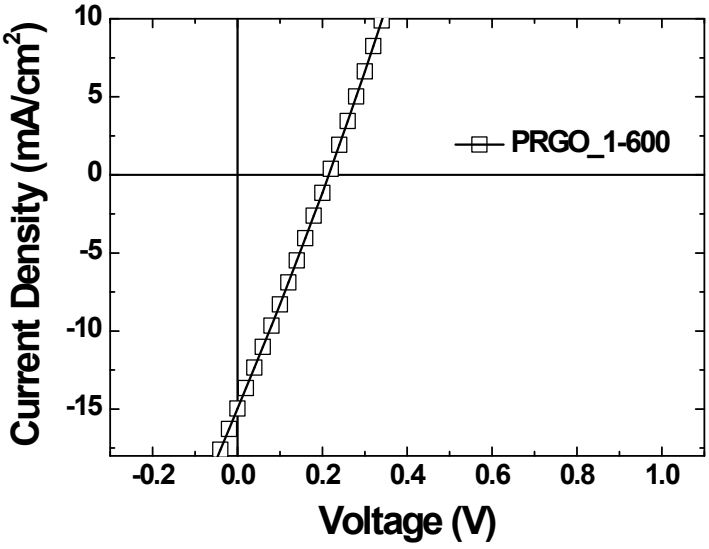

Fig. S3. J-V plot of PeSC employing PRGO_1-600.

Although the reduction of the AN concentration could induce the better characteristics of the PRGO as a HTL, AN concentration reduced further than 2 wt% of AN precursor significantly degraded the device-performance. As shown in Fig. S3, the PRGO synthesized by 1 wt% of AN precursor (PRGO_1-600) could not effectively rectify the photocurrent of the PeSCs. This resulted from the poor dispersibility of the PRGO in the solvent due to the lack of the grafted PAN contents.

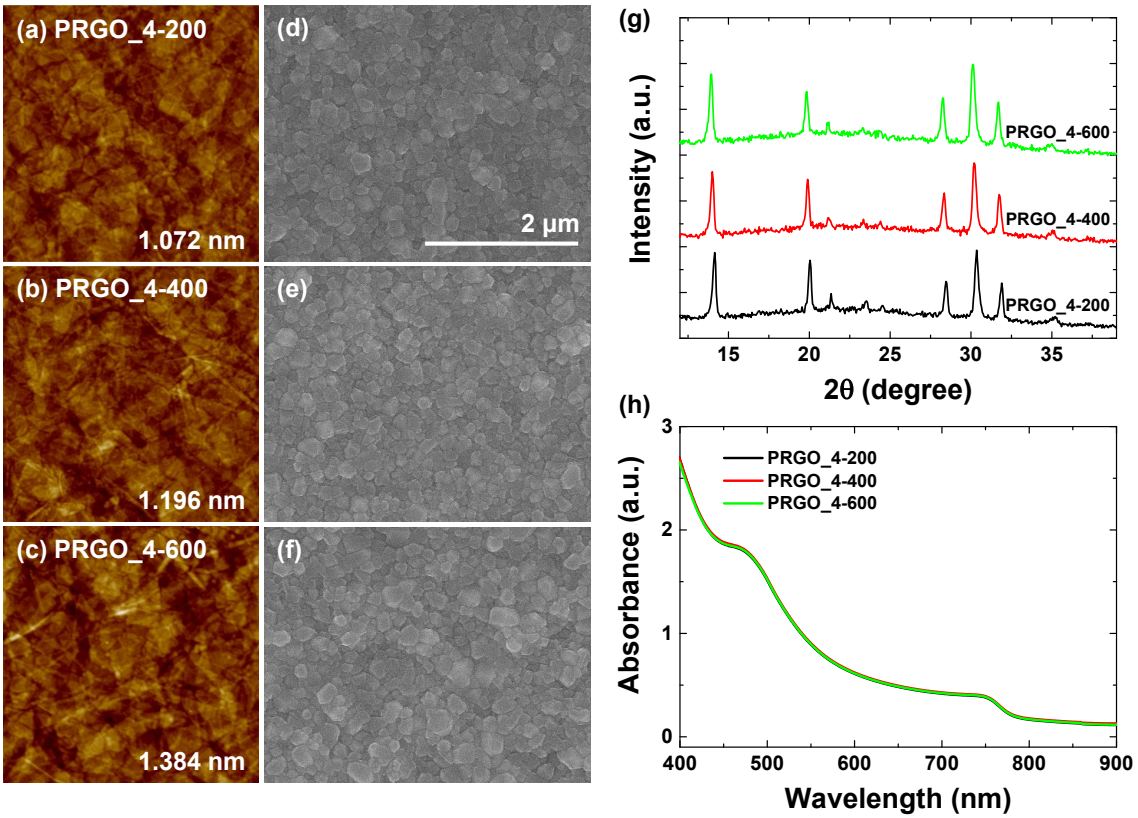

Fig. S4. (a-c) AFM topographic images with corresponding roughness of PRGO_4-200, PRGO_4-400, and PRGO_4-600 on ITO substrates. (d-f) Top-view SEM images, (g) XRD patterns, and (h) absorbance of $MAPbI_3$ films on PRGO_4-200, PRGO_4-400, and PRGO_4-600.

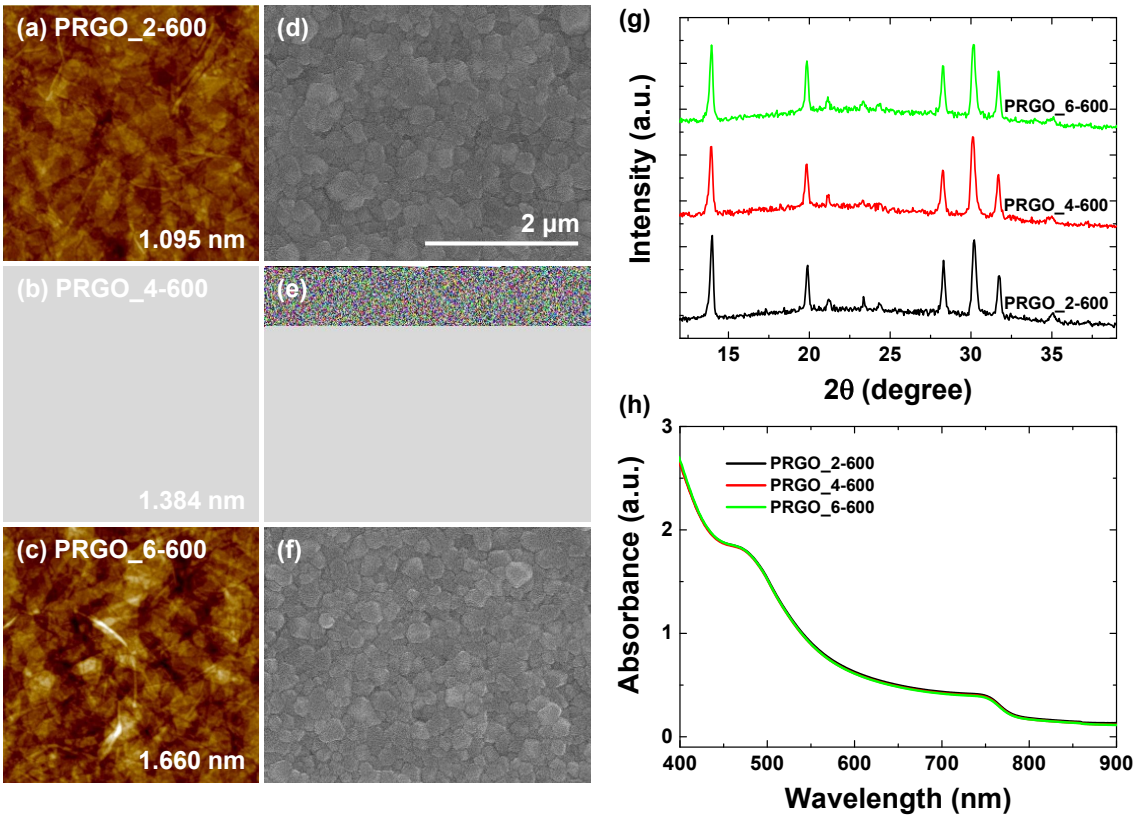

Fig. S5. (a-c) AFM topographic images with corresponding roughness of PRGO_2-600, PRGO_4-600, and PRGO_6-600 on ITO substrates. (d-f) Top-view SEM images, (g) XRD patterns, and (h) absorbance of $MAPbI_3$ films on PRGO_2-600, PRGO_4-600, and PRGO_6-600.

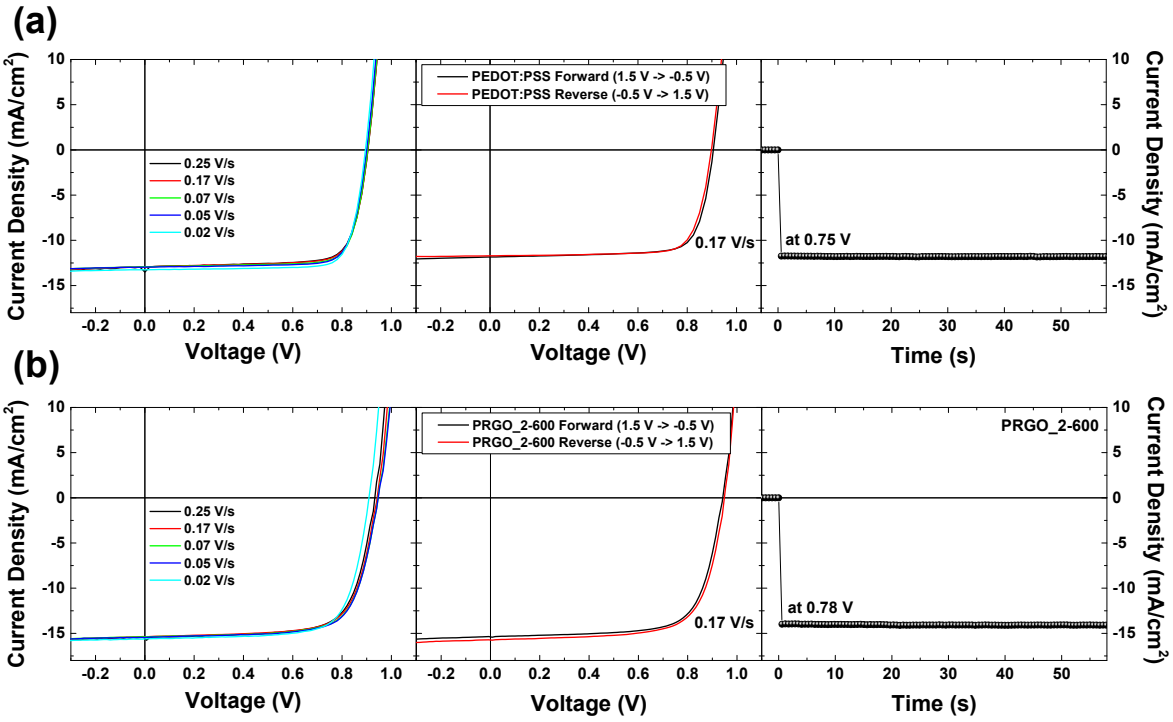

Fig. S6. J-V characteristics depending on sweep rates and directions, and current transients measured at respective maximum voltages for PeSCs based on (a) PEDOT:PSS and (b) PRGO_2-600.

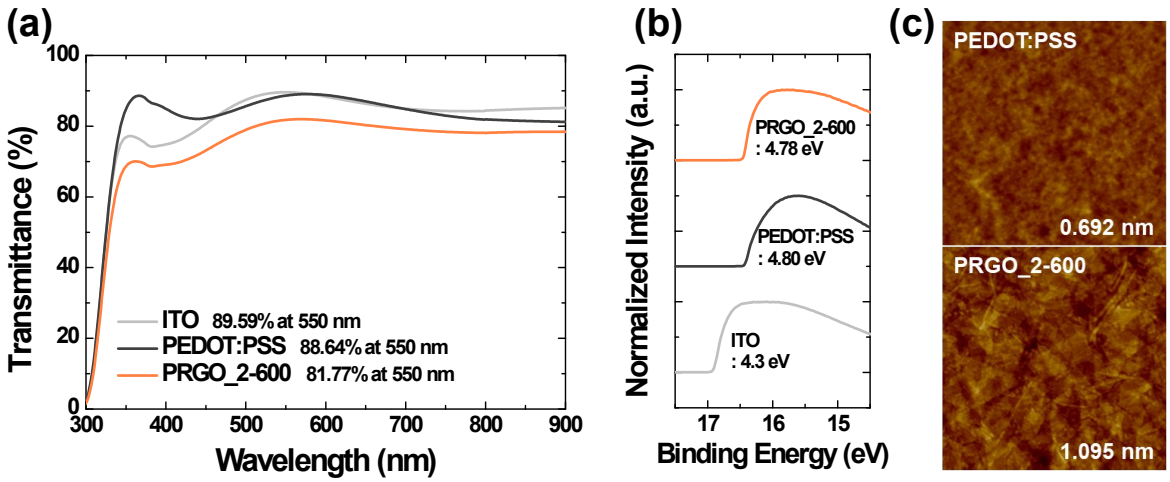

Fig. S7. (a) Transmittance and (b) UPS spectra in secondary electron cutoff region of ITO, ITO/PEDOT:PSS, and ITO/PRGO_2-600. (c) Topological AFM images with corresponding roughness of ITO/PEDOT:PSS, and ITO/PRGO_2-600.

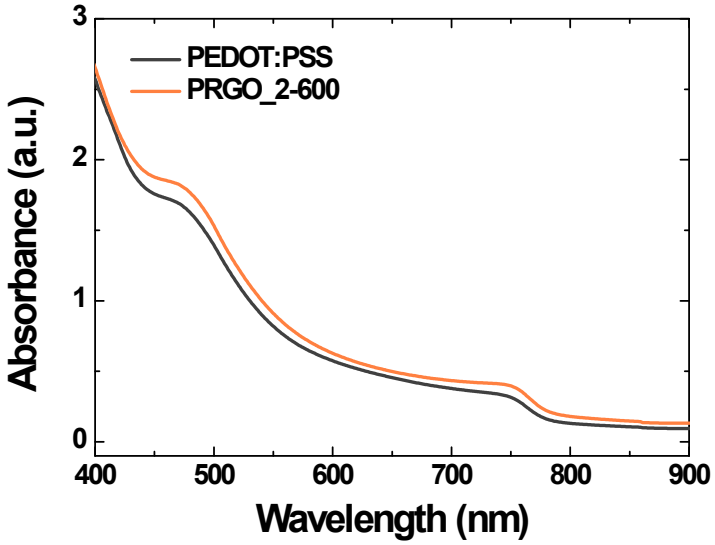

Fig. S8. Absorbance spectra of PEDOT:PSS/$MAPbI_3$ and PRGO_2-600/$MAPbI_3$.